Supplement to

A QUANTITATIVE SYSTEM PHARMACOLOGY COMPUTER MODEL FOR COGNITIVE DEFICITS IN SCHIZOPHRENIA

Hugo Geerts [1,2] , Patrick Roberts [1,3], Athan Spiros [1]

[1] In Silico Biosciences, Berwyn , Pennsylvania

[2] Perelman School of Medicine, Univ of Pennsylvania

[3] OHSU, Portland Oregon

METHODS.

1. The Receptor Competition Model

An important issue for any modeling of clinical situations is the target engagement of the antipsychotics at their respective clinical dose. To calculate the functional free concentration of the drug, we use the receptor competition model, a set of ordinary differential equations that describe the competition between neurotransmitter, drug, its metabolite and a possible radiotracer [1].

Basically the receptor competition model is a set of ordinary differential equations that describes the time-dependent changes in pre- and postsynaptic receptor activations, neurotransmitter and drug levels in the synaptic cleft and amount of binding to different receptors. We use a series of differential equations that simulate the binding of up to four agents at pre- and postsynaptic receptors based upon their respective affinities under realistic presynaptic firing conditions of the endogenous neurotransmitter [1].

$$\partial[R_n]/\partial t = k_{on}^n \times [NT] \times [R_f] - k_{on}^n \times K_d^n \times [R_n] \qquad \textit{Eq S1}$$

Where n is for neurotransmitter. Similar equations are used for drug1, drug2 and tracer. R_f denotes the level of free receptor; k_{on} is the on-rate (usually diffusional controlled if not experimentally determined) and K_d is the dissociation constant.

Exponential decay of the neurotransmitter is defined as

$$[NT](t) = [NT(0)]*\exp(-t \ln(2)/\text{halflife}) \qquad \text{(Eq S2)}$$

where *halflife* is the half-life of the decay process. This is modulated by transporters (in the case of DA, 5-HT and NE) or enzymes (Acetylcholinesterase for Ach and Catechol-O-Methyl transferase for DA and NE).

The amount of presynaptic receptor activation which occurred 150 ms before the current release event then determines the amount of new release as follows

$$release_{new} = release_0 \left[1 + relScale \left(1 - 2 \frac{recAct^{\,relSens}}{recAct^{\,relSens} + normBound^{\,relSens}} \right) \right] \quad \text{Eq S3}$$

where $release_0$ is the base release amount, *relScale* is the maximum relative change for release, *recAct* is the receptor activation at the specified time in the past, *relSens* is the sensitivity to presynaptic receptor (lower values create a shallow response and higher values create a sharp difference between activation levels), and *normBound* is the amount of normal presynaptic binding that one would expect in the tonic case (i.e. when *recAct* equals *normBound*, the new relase equals the baseline release amount). We calibrate the parameters so that the coupling of presynaptic D2R activation to dopamine release reflects actual experimental data (as seen in Results section). All differential equations are solved with a fourth-order Runge-Kutta method with a time step of 0.01 msec.

In addition, the release can be modulated by a depression or facilitation mechanism [2]. Instead of using internal Ca^{++} levels to determine dopamine release, we consider the facilitation and depression of dopamine release based solely on the amount of time elapsed since the previous firing using a phenomenological equation. Thus, the amount of dopamine released is based both on the history of firing and the activation level of the presynaptic D2 autoreceptors. If we denote the time of the n^{th} firing by t_n, then the release amount is modified based on all previous firings as follows

$$release_{new} = release \left(1 + \sum_{i=1}^{n-1} w_f \exp\left[-k_f (t_n - t_i) \right] - w_d \exp\left[-k_d (t_n - t_i) \right] \right) \quad \text{Eq S4}$$

where w_f is the facilitation weight, w_d is the depression weight, k_f is the decay rate of facilitation and k_d is the decay rate of depression. All these parameters can be calibrated to experimental data if they are available.

The simulation is initiated by first finding the equilibrium given a constant amount of free dopamine at 500 nM. The simulation is then run for a transitory time of 5 seconds at the tonic firing rate of 4 Hz.

All the parameters that describe the presynaptic neurotransmitter physiology are calibrated with preclinical experiments using rapid-cyclic fast voltammetry on levels of neurotransmitters [3, 4].

We use this model in two steps. First, the functional free intrasynaptic concentration of the drugs is determined by simulating the competition between total active moiety (including the active metabolite) and tracer at the postsynaptic D_2R in a PET radiotracer displacement study [5]. For cortical drug concentrations we use tracer displacement data of various antipsychotics on FLB417 [6]. Using the competition model between neurotransmitter, drug and tracer for binding at the postsynaptic receptor, we can determine the drug concentration that corresponds to a clinically measured radiotracer displacement. This value for the drug concentration is the free and functional intra-synaptic concentration that is dependent upon the PK properties of the drug and is used in further calculations. For all the studies we assume steady-state plasma and target engagement values.

Second, we can then use this free functional concentration of the active moiety to calculate the postsynaptic receptor activation in other non-dopaminergic D_2 synapses, dependent upon the affinity of the drug, its metabolite and the endogenous neurotransmitter (such as 5-HT or Ach). The change in the appropriate postsynaptic receptor activation is then used to derive the change in voltage-mediated ion channels that drive the excitability of the network (see below).

2. Calibration of the serotonergic synaptic cleft model

The serotonergic synaptic cleft model is calibrated using both in vivo experimental data on free 5-HT levels in preclinical animal models and human imaging data using specific radiotracers. The preclinical data measure the free serotonin levels during forced firing frequency of the presynaptic terminals and therefore probe the effect of presynaptic 5-HT1B autoreceptor coupling and

facilitation/depression on the release of 5-HT. 5-HT1B is the most important autoreceptor for most projection serotonergic neurons, while 5-HT1A is the major autoreceptor regulating DR firing [7].

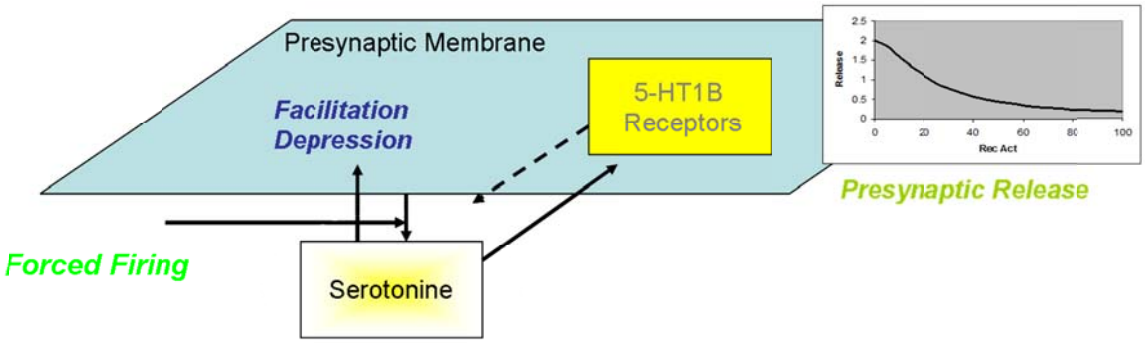

Fig.S1 Processes involved in measuring free serotonin levels by fast cyclic voltammetry. In this particular experiment only the change in free 5-HT, but no postsynaptic activation level is measured. The experimental setup forces high frequency firing on the presynaptic nerve endings and allows calibration of the different presynaptic parameters that regulate the coupling between presynaptic autoreceptor activation, firing history and subsequent neurotransmitter release. Some parameters, such as 5-HT release and half-life are constrained by biological limits. (see further below)

For the proper validation we use fast cyclic voltametry data in mouse slices substantia nigra [8, 9] which have been shown to be rich in serotonin innervation. Free 5-HT levels are measured after forced firing. This ensures that only the effect at the presynaptic 5-HT1B autoreceptor is measured.

An important issue is how much of the intrasynaptic 5-HT these fast cyclic voltammetry probes are detecting. Modeling studies of the glutamate synapse [10] suggest that intrasynaptic levels can be between 1x and 20 times the measured extrasynaptic levels.

Because it is important to know the free 5-HT level in the human situation, the strategy is to systematically vary the ratio of extra- vs. intrasynaptic free 5-HT, for each of these ratios, calibrate the 'mouse' 5-HT synapse, and then select the best ratio that has the highest correlation between the output of the synaptic model and actual clinical data on human imaging experiments (see below).

Using the above-mentioned values for 5-HT1B we adjusted the parameters of the synaptic cleft until we got a good correlation between model outcomes and experimental values; and did this for different ratios of intra-synaptic over extra-synaptic free 5-HT.

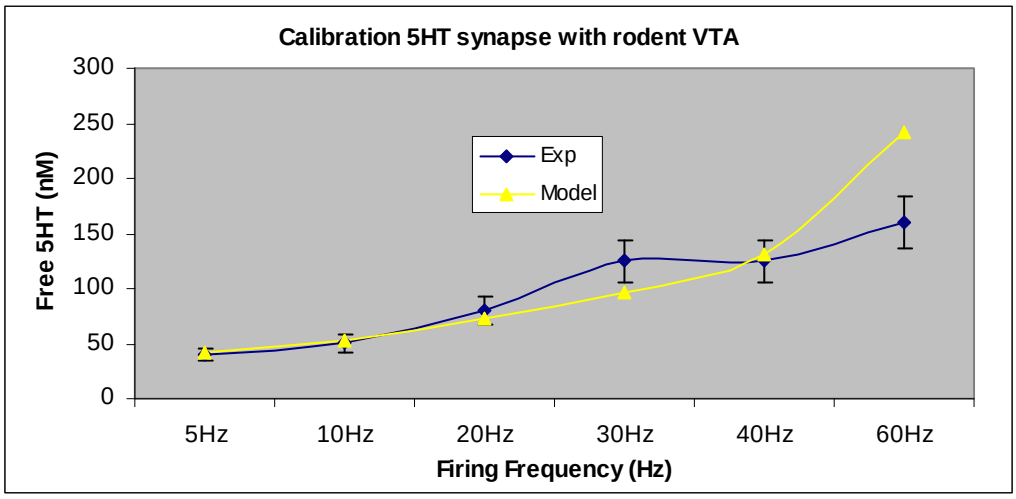

Fig. S2 Correspondence between model outcomes and experimentally reported values in the mouse substantia nigra [8]under forced firing frequencies. The model parameters of the serotonergic synapse are adjusted to show a good correlation with the experimental data. This particular calibration is for the situation where the extrasynaptic concentration equals the intrasynaptic free level of 5-HT. Similar curve fittings are done for other situations (from 1x to 10x the measured extrasynaptic levels). Because the in vivo serotonergic firing frequency is around 1Hz, we took great care to fit the low end of the frequency datapoints.

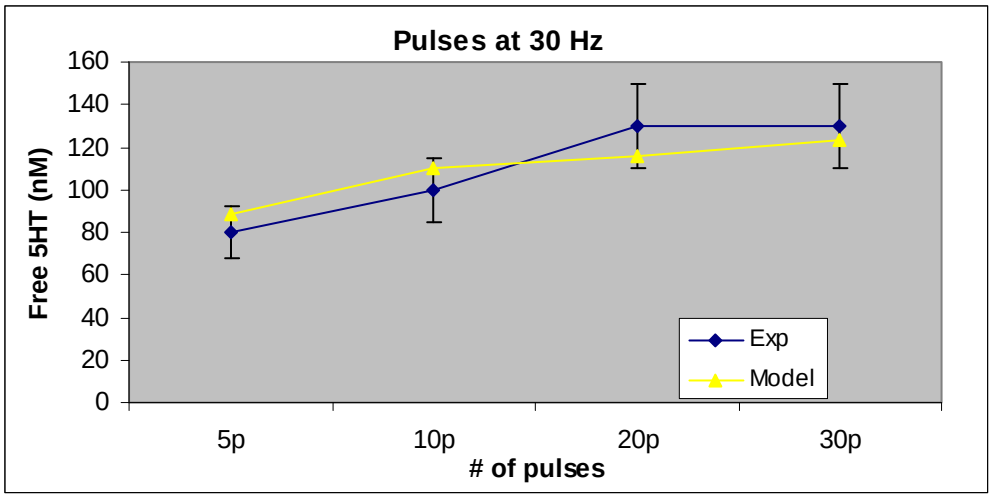

Fig. S3 Correspondence between model outcomes and experimentally reported values in the mouse SN [9] under forced firing frequencies. The model parameters of the serotonergic synapse are adjusted to show a good correlation with the experimental data. This particular calibration is for the situation where the extrasynaptic concentration equals the intrasynaptic free level of 5-HT. Similar curve fittings are done for other situations (from 1x to 20x the measured extrasynaptic levels).

The following table then shows the values of the adjustable parameters of the serotonergic synapse (for a definition of the parameters, see Methods Section) for each of the cases that refer to the ratio between intrasynaptic and extrasynaptic 5-HT levels.

The calibration is performed using mouse data; however we are interested in the human situation. Unfortunately we don't have access to free 5-HT levels in human brain. The closest we can get is the result of PET radiotracer displacement imaging studies using 5-HTR specific radio-tracers. The strategy is to select the parameter set in Table 2 within the 1x-10x range that best fits the displacement of 5-HT2AR tracers in schizophrenia patients treated with certain antipsychotics with affinity for the 5-HT2AR.

The following table lists the different published imaging studies in schizophrenia and the effect of antipsychotics on displacement of specific 5-HTR radiotracers. In some publications also the corresponding D2R occupancy is given; in all the other cases we use values of raclopride D2R displacement obtained from independent imaging trials using the same clinical doses.

Receptor	Tracer	Intervention	Effect in imaging	Note	Ref
5-HT1A Receptor	WAY100635	30 mg aripiprazole	5-HT1AR occupancy 16%	D2R occupancy >90%	[11]
5-HT2A Receptor	Altanserin	6 month quetiapine treatment	block between 60-70%		[12]
5-HT2A Receptor	Setoperone	30 mg aripiprazole	5-HT2AR occupancy 58%	D2R occupancy >90%	[11]
5-HT2A Receptor	Setoperone	200 mg clozapine, 100-600 mg chlorpromazine, amisulpride	Occupancy >80% for chlorpromazine, >90% for clozapine, 0-10% for amisulpride		[13]
5-HT2A Receptor	Setoperone	10-100 mg loxapine	Occupancy between 27-100%		[14]

5-HT2A Receptor	Setoperone	10 mg amoxapine	Occupancy between 90-100%		[15]

Table S1. Imaging studies with antipsychotics showing displacement of 5-HT2A specific tracers because of the endogenous affinity of the drugs for the 5-HT2AR.

The imaging studies with WAY100635 after aripiprazole in schizophrenia patients suggest a low receptor occupancy of about 16% despite a high affinity of aripiprazole for this receptor (3-4 nM), where it is documented to be a partial agonist [16]. As the authors acknowledge in their discussion, this is likely due to the fact that the binding affinity in vitro is measured using a labeled agonist (8-OH-DPAT), while the imaging experiment uses the antagonist WAY100635. Agonists and antagonist probably probe different states of the receptor, i.e. active open state vs. closed desensitized state [17, 18]. For this reason we eliminated this 5-HT1A imaging study leaving us with seven studies on the 5-HT2AR.

Binding studies using radio-active tracers usually probe the low-energy desensitized state [17]. In this study however we need to use the association kinetics for the active state, as the experimental conditions studies the effect of released serotonin on the presynaptic physiology following activation of the 5-HT1B autoreceptor. Also, in all other simulations, we study the effect of interventions on the active state of pre- and postsynaptic receptors.

We use the following values for the different 5-HTR.

Affinity of 5-HT for	**Antagonist (nM)**	**Agonist tracer (nM)**	**Low affinity (nM)**	**EC_{50} (nM)**	**Reference**
5-HTT	*258.73*				
5-HT1A	3.17	166.00	102	74.13	[19]

5-HT1B	23.50	4.32		8.51	[20]
5-HT1D	3.40	3.68		1.29	[21]
5-HT1E	*7.00*	7.53			
5-HT1F	15850	10.00			
5-HT2A	11.55	21.00		30.20	[22]
5-HT2B	2.82	8.71		2.82	[22]
5-HT2C	15.50	5.02		1.51	[22]
5-HT3	593.00	N/A		4200	[17]
5-HT4	316.22	*6.30*		20.00	[23]

Table S2. Binding affinity, association constants and functional EC_{50} values for 5-HT with regard to the different 5-HTR subtypes (publicly available data). Italic values are for rodent species, all other values are for humans.

We can calculate functional brain concentration of the antipsychotic drugs using published data on raclopride D2R displacement. For each of the conditions mentioned above, we can then simulate the displacement of the tracers setoperone or altanserin by the appropriate functional brain concentration of the antipsychotic, given its known affinity for the human 5-HT2AR. Because the amount of tracer displacement results from a complex interaction between tracer, drug and serotonin, it will depend upon the level of free 5-HT. A proper alignment with the clinical imaging data will gives us a better idea of the actual 5-HT levels that are driving the 5-HT dynamics at least in schizophrenia patients. We further assume that these values can be extrapolated to normal healthy subjects, as schizophrenia is mostly associated with a dopamine dysfunction [24].

The following table gives the affinities of the radiotracers commonly used in human PET imaging studies

Receptor	Tracer	Affinity	Reference
5-HT1A	WAY100635	0.3 nM	[25]
	MPPF	3.1 nM	[26]
5-HT2A	Altanserin	0.3 nM	[27]
	Setoperone	0.43 nM*	[28]
5-HT4	SB207145	0.59 nM	[29]

Table. S3. List of different radiotracers and their affinities for the respective receptors. All entries are human based affinities, except for setoperone. .

As mentioned before, we first determine the functional brain concentration of the compounds using raclopride tracer imaging experiments and their known affinities against the presynaptic D2SR and the postsynaptic D2L receptor in a primatized model of the striatal serotoninergic synapse [1].

Ideally one would like to quantify the binding of a specific radio-tracer before and after neuroleptic treatment to correct for any individual baseline variability of the receptor. Although this is possible with our model, it is usually difficult in the clinical setting so that many studies define a binding index (Eq 8) compared to a normal control population

$$BindIndex = 100 * (1 - \frac{(A_m - Cer_m)_{patients}}{(A_m - Cer_m)_{controls}}) \qquad \text{Eq S5}$$

Where A_m and Cer_m are the specific radio-active signal in the region of interest (i.e. striatum and cerebellum, respectively).

We used radio-tracers at a concentration of 10 pM and the corresponding values for K_d from Table 5. The K_d of raclopride for the D2 receptor is 1.3 nM [30, 31]. We defined the apparent receptor occupancy as

$$AppOcc = 100 * (1 - \frac{R_{drug}^{tracer}}{R_{control}^{tracer}}) \qquad \text{Eq S6}$$

where R_{drug} and $R_{control}$ are the receptor tracer occupancies respectively in the presence or the absence of the drug.

The affinities of the drugs for the different receptors are shown in the following table.

Drug	**D2**	**5-HT1a**	**5-HT1b**	**5-HT2a**	**Conc (nM)**
amisulpride	1.3	10000	10000	2000	**9**
amoxapine	18	10000	10000	0.5	**120**
aripiprazole	pa3.3 (70%)	pa3.85 (70%)	830	21.8	**85**
chlorpromazine	5.5	2115	1498	2.05	**38**
clozapine	220	118	398	8.3	**200**
clozapine-metabolite	115	13.9	406.8	10.9	**50**
loxapine	11	2456	388	6.6	**80**
quetiapine	406	431	2050	264	**450**

Table.6 Affinity of drugs (k_i) measured using competition with labeled antagonists. The last column shows the obtained free functional concentrations for the compound that match the reported clinical raclopride striatal D2R displacements. All compounds are antagonists except where noted as ***pa X (Y%)*** *where X is the EC_{50} of the compound in nM and Y is the E_{max} of functional activation (usually expressed as a percentage of the full agonist activation level).*

Because raclopride displacement is measured functionally it takes into account many confounding issues such as blood-brain barrier transport and free fraction etc. and reflects the actual true concentration of the drug.

Using the functional concentrations of the antipsychotics derived from the raclopride displacement studies the appropriate affinities of the schizophrenia drugs against the 5-HTR, we then simulated the displacement of 5-HT2AR tracer for the seven clinical cases and compared the outcomes with the clinically reported data.

For each of the ratios of intrasynaptic vs extrasynaptic 5-HT levels we used the appropriate parameters of the calibration to run the seven clinical imaging data points. The residue is calculated as

$$\mathrm{Re}\,s = \sum_{i=1}^{7} \frac{(Dis_m^i - Dis_e^i)}{Dis_m^i} * (Dis_m^i - Dis_e^i) \qquad \text{Eq. S7}$$

Where Dis^i_m is the model displacement and Dis^i_e is the experimentally measured displacement.

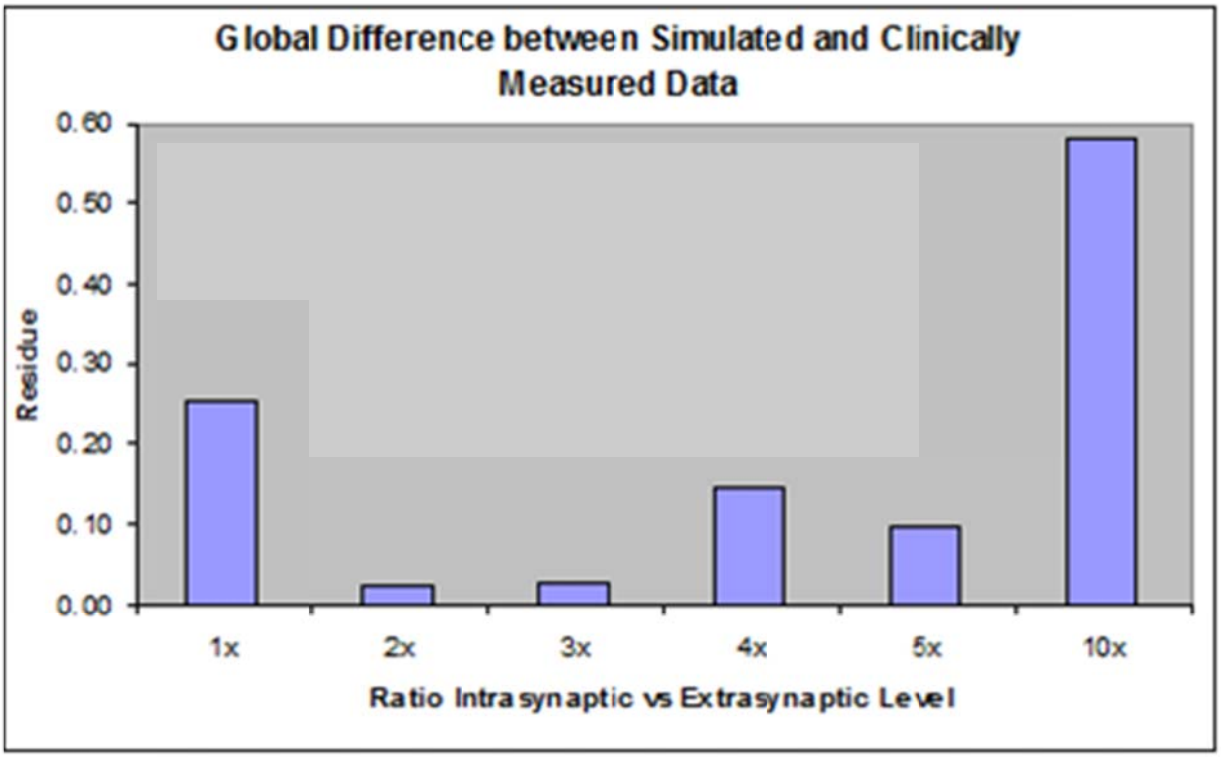

Fig S4. Residu between experimentally measured displacement in human patients under different conditions and the receptor competition model outcome for different ratios of extra- over intrasynaptic free 5-HT concentrations. The results suggest that a ratio of 2 best reflects the human 5-HT synapse dynamics.

3. The Cortical Network

We extended a biophysically realistic model of a network comprised of 20 four-compartment pyramidal cells and 10 two-compartment GABA interneurons [32, 33] with the receptor physiology of 18 different dopaminergic, serotonergic, noradrenergic, and cholinergic receptors (Fig 1). We only discuss here the changes relative to the published paper. Basically this network is a smaller version of the network used for simulating cognitive decline in Alzheimer's disease [4], but with implementation of a different schizophrenia-type pathology.

An $mGluR_5$-dependent delayed afterdepolarization current that can increase the spiking rate of pyramidal cells for several seconds was implemented as an alpha function in the model with a time constant similar to the observation in [34]. Based on insights from the relative number of pyramidal cells and interneurons [33, 35], 40% of the interneurons synapsed with other GABA interneurons, but not with pyramidal cells.

A stimulus is initiated by injecting a current at t=2000 msec which starts the firing of the target pyramidal cells. Without further stimuli, this synchronized firing pattern goes on for a certain amount of time before it gets degraded by the background noise and the interference of the distractor neurons. This time span, called the working memory span, is usually in the range of 4-10 sec and corresponds to the time a certain pattern is held in working memory [36].

To calculate this time span, we first divide the time axis in bins of 200 msec and count the number of neurons firing in that time window and determine the time points where this number exceeds M/2, where M is the number of neurons stimulated at t=2000 msec (M=10 for the network). The time difference between these two transition points is the memory span (Fig 1B).

Receptor	**Physiological implementation**	**Reference**
Dopamine D1R	Increases NMDA, decreases AMPA and increases GABA conductance	[37]
Dopamine D2R	Presynaptic autoreceptor; modulates AMPAR on pyramidal cells	[38]
Dopamine D4R	Affects AMPA-R functions	[39]
Serotonin 5-HT1A	Affects Na-currents	[40], [41, 42]
Serotonin 5-HT1B	Presynaptic autoreceptor in 5-HT synapse	[42]

Serotonin 5-HT2A	Affects Na and High Threshold Ca-currents	[43]
Serotonin 5-HT3	Modulates GABA conductance	[44]
Serotonin 5-HT4	Affects serotonergic firing rates; affects K_{dr} and K_s and GABA in pyramidal cells	[45, 46],
Serotonin 5-HT6	Modulates levels of ACh, NE and DA	[47]
Adrenergic Alpha2A	Modulates K^+ conductance on inhibitory interneurons	[48]
Muscarinic M1R	Cl leak in MSN & K_{dr} in pyramidal cells	[49] [50]
Muscarinic M2R	Presynaptic autoreceptor for cholinergic synapses;	[51] [52]
Nicotinic $\alpha 7$ AChR	Increases presynaptic Glu release, increases interneuron excitability	[53, 54]
Nicotinic $\alpha 4\beta 2$ AChR	Increases presynaptic GABA release	[55]

Table S4. List of receptors effects implemented in the model, their localization and possible physiological effect. In addition, the model takes into account the physiology of NMDA, AMPA and GABA-A receptors and of mGluR2 although none of the antipsychotics directly interact with these receptors [53].

4. Implementation of receptor pharmacology

This section deals specifically with the implementation of dopaminergic neurotransmission physiology. Other neuromodulatory processes (serotonergic. cholinergic, noradrenergic) are implemented using similar approaches. In general, we assume a linear normalized relationship between receptor activation and biological effect on physiological responses such as $X_Y^{eff} = \frac{X_Y^A - X_Y^C}{X_Y^C}$; where $X_Y{}^A$ and $X_Y{}^C$ are the actual activation levels of receptor X subtype Y (for instance D_1) after treatment (A) and the untreated (placebo) control levels (C).

$$g^{*}_{NMDA} = g_{NMDA} \times (1 + Param_{NMDA}^{D_1} \times \frac{D_1^{A} - D_1^{C}}{D_1^{C}}) \qquad \text{Eq S8}$$

$$g^{*}_{AMPA} = g_{AMPA} \times (1 + Param_{AMPA}^{D_1} \times \frac{D_1^{A} - D_1^{C}}{D_1^{C}}) \qquad \text{Eq S9}$$

$$g^{*}_{GABA} = g_{GABA} \times (1 + Param_{GABA}^{D_1} \times \frac{D_1^{A} - D_1^{C}}{D_1^{C}}) \qquad \text{Eq S10}$$

The D_2S receptor is a presynaptic autoreceptor in the cortex and regulates the activity level of the cortical D_1 and D_4 receptors [56]. This is taken into account by the cortical dopamine receptor competition model. Furthermore, D_2R is located postsynaptically on pyramidal cells and modulates EPSP [38, 57] through an early AMPA mediated process and a late GABA mediated process. D2R activation modulates AMPA conductance according to

$$g^{*}_{AMPA} = g_{AMPA} \times (1 + Param_{AMPA}^{D_2} \times \frac{D_2^{A} - D_2^{C}}{D_2^{C}}) \qquad \text{Eq S11}$$

where D_2^{A} and D_2^{C} are actual D2 activation levels for treated subjects and healthy control levels, respectively and $Param_{AMPA}^{D2}$ is an adjustable parameter.

Dopamine D_4R activation affects AMPA-R similarly but only on interneurons [39]. D4R activation increases the AMPA channel conductances such that

$$g^{*}_{AMPA} = g_{AMPA} \times (1 + Param_{AMPA}^{D_4} \times \frac{D_4^{A} - D_4^{C}}{D_4^{C}}) \qquad \text{Eq S12}$$

where D_4^{A} and D_4^{C} are actual D2 activation levels for treated subjects and healthy control levels, respectively and $Param_{AMPA}^{D4}$ is an adjustable parameter.

5. Calibrating the model

First the pathology of schizophrenia is implemented based on the observed changes in patients, a hypodopaminergic tone on the cortical D_1R [32], an NMDA hypofunction [58, 59] that is documented by a hypocortical-hyperstriatal imbalance in metabolic imaging [60], a GABA deficit more specifically in the chandelier interneurons [61] but applied here to the

interneurons in the network, and a more noisy background signal [62]. This leads to a cognitive deficit in schizophrenia patients which is dependent upon the clinical readout, but on average is 1.5 standard deviations lower than healthy controls [63-65].

We will first explore the sensitivity of the network model outcome as a function of these four parameters to identify the possible biological drivers of pathology-driven network changes. We then simulate the effect of 100 different virtual 'normal subjects' that have variable values around the optimal values. Based on the observation that schizophrenia patients perform at a level that is about 1.5 standard deviations lower than normals on a number of cognitive tests, we can then determine the minimal changes in the four parameters that corresponds to a network cognitive outcome as determined by this difference.

In a second step, the remaining free biological coupling factors such as $Param_{AMPA}^{D4}$ are further calibrated using clinical data on the N-back working memory test as reported in schizophrenia patients, healthy controls with anticholinergics or COMT inhibitors and stratified according to the COMT genotype. Table 1 lists the clinical observations on diverse interventions used for calibrating the cortical cognitive network.

Subjects	*Treatment*	*COMT genotype*	*2-Back WM performance (% correct)*
Schizophrenia	*Placebo*	*COMT Met/Met*	*49.8*
Schizophrenia	*Placebo*	*COMT Val/Met*	*42*
Schizophrenia	*Placebo*	*COMT Val/Val*	*43.4*
Schizophrenia	*Perphenazine 8, Ziprasidone 80 Quetiapine 600*	*COMT Met/Met*	*61.6*
Schizophrenia	*Clozapine 250, Haldol 10, Quetiapine 700, Risperidone 6*	*COMT Val/Met*	*40.1*
Schizophrenia	*Haldol 10, Risperidone 6*	*COMT Val/Val*	*43.6*
Schizophrenia	*Olanzapine 20*	*COMT Met/Met*	*73*

Schizophrenia	*Olanzapine 20*	*COMT Val/Met*	*56.6*
Schizophrenia	*Olanzapine 20*	*COMT Val/Val*	*47.6*
Healthy volunteers	*Placebo*	*N/A*	*81*
Healthy volunteers	*Mecamylamine*	*N/A*	*79*
Healthy volunteers	*Scopolamine*	*N/A*	*69*
Healthy volunteers	*Mecamylamine & scopolamine*	*N/A*	*61*
Healthy volunteers	*Placebo*	*COMT Met/Met*	*83*
Healthy volunteers	*Tolcapone*	*COMT Met/Met*	*82*
Healthy volunteers	*Placebo*	*COMT Val/Val*	*76*
Healthy volunteers	*Placebo*	*COMT Val/Val*	*81*

Table S5. Clinical changes in 2-back working memory performances for a number of therapeutic interventions. The data are taken from studies in schizophrenia patients [66, 67] and healthy controls [68] with cholinergic changes and with COMT modulation [69]. For experiments where no COMT genotype data are available, we assume a COMT MV genotype.

The calibration of the network is performed using 'Design of Experiment' (DOE) statistical techniques, rather than OFAT (one Factor At a Time). OFAT techniques, besides being computationally intensive also are unable to detect interaction between parameters to be calibrated [70]. DOE techniques are computationally effective and provide a sound statistical approach to identify the driving parameters.

A good robust approach uses 2n simulations, where n is the number of free parameters, compared to 2^n for a full OFAT design [71] .

A [2n x n] matrix **A** is then constructed with elements a_{ij}, where i is the run number (1..14) and j = the calibration parameter (1..7) and defined by

a_{ij} = Max(j) if e_{ij} = 'P' and a_{ij} = Min(j) if e_{ij} = 'M' Eq S13

An [n x 1] row Average+ is constructed with elements $\text{Average+}_j = \sum_{i=1}^{14} Outcome[i] \times Pos_{ij}$

where Pos_{ij} = 1 if e_{ij} = 'P' and Pos_{ij} = 0 if e_{ij} = 'M' Eq S14

Similarly, an [n x 1] row Average- is constructed with elements

$$\text{Average-}_j = \sum_{i=1}^{14} Outcome[i] \times Neg_{ij} \qquad \text{Eq S15}$$

where $Neg_{ij} = 0$ if e_{ij} = ’P’ and $Neg_{ij} = 1$ if e_{ij} = ’M’ Eq S16

The Pareto-effect, Par_j (j=1..n), is simply the difference Average+_j - Average-_j and indicates both the strength and the sign of the gradient towards the optimum.

The next iteration will use this information to adjust the range of the parameters, until the Pareto effects become so small that a more detailed surface response is initiated.

RESULTS

1. Implementation of schizophrenia pathology

We first studied the sensitivity of the network outcome on the different processes that are implicated in the schizophrenia pathology. Fig 2 shows the effect of changing the NMDA-R conductance in a range of 25%, the GABA conductance in a range of 10%; the D_1R activation between 7 and 37% and the noise level between 36 and 84%. In terms of outcome variability (range of outcomes divided by average outcome) the greatest effect was observed for NMDA changes (0.63); followed by GABA changes (0.43), noise (0.26) and D1R activation level (0.16).

In general, the outcome decreases when introducing the pathology. For instance increasing the noise leads to a monotonic decrease of working memory span. However, for changes in the NMDA conductance, the maximum is around 0.92, suggesting that the first decrease leads to an improvement, probably due to the relatively bigger effect on the excitatory-inhibitory glutamate synapses that tend to decrease the inhibitory tone and lead to a disinhibition. After a certain value is reached the decrease in excitatory-excitatory glutamate strength tend to reduce network activity.

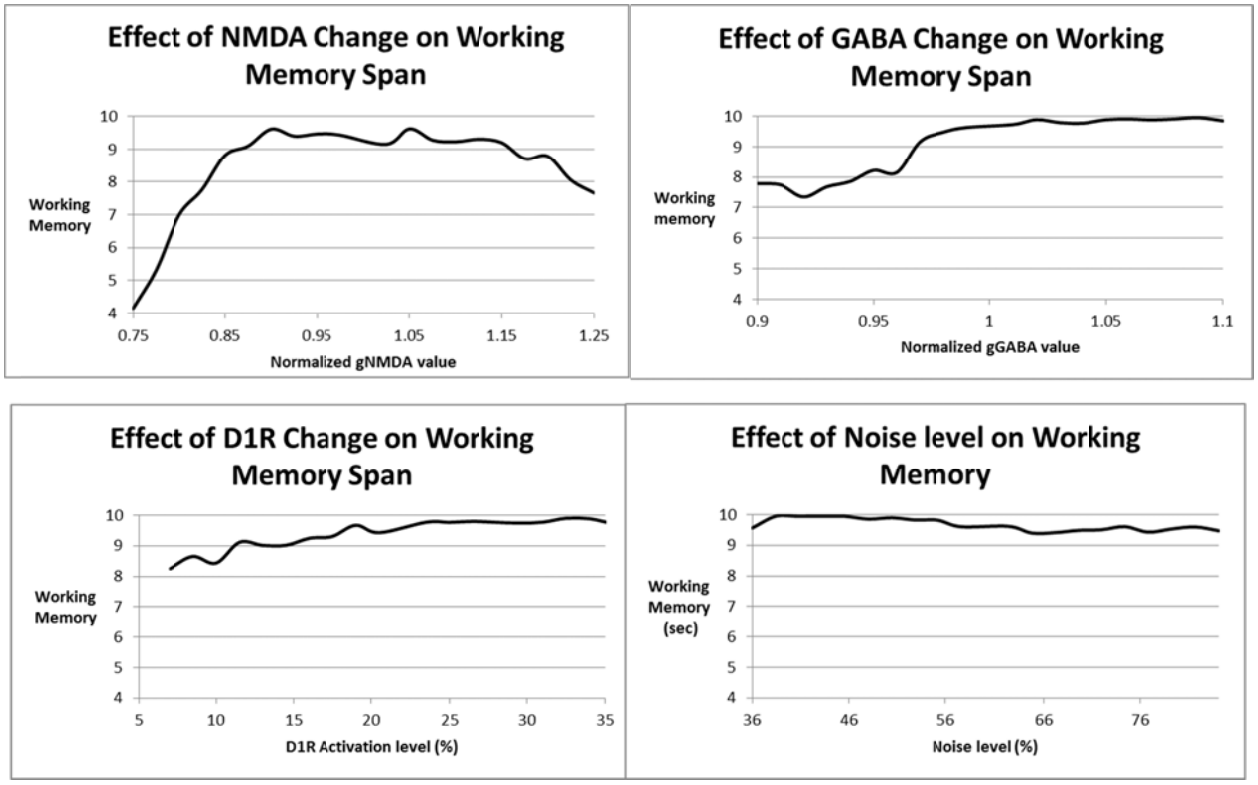

Fig. S5. Sensitivity analysis of the different parameters involved in the schizophrenia pathology to the outcome of working memory span. The basal D_1 activation level is 22% and the basal noise level is 60. It turns out that changes in the NMDA conductance have the biggest effect on the outcome.

2. Calibration of the cortical model

For the calibration of the remaining free biological coupling parameters we proceeded to the Design-of-Experiment approach to constrain the remaining free values for the biological coupling parameters. The purpose was to optimize the correlation between the model outcome and the actual clinical performance on the 2-Back working memory test for the 17 different interventions listed in Table 1. We used a 2n Design-of-Experiment approach where we first determined the processes that impacted most the correlation value (where n=7 is the number of free parameters). When the Pareto plots indicated no further improvement we switched to a local maximum search.

References

1. Spiros, A., R. Carr, and H. Geerts, *Not all partial dopamine D(2) receptor agonists are the same in treating schizophrenia. Exploring the effects of bifeprunox and aripiprazole using a computer model of a primate striatal dopaminergic synapse.* Neuropsychiatr Dis Treat, 2010. **6**: p. 589-603.
2. Montague, P.R., et al., *Dynamic gain control of dopamine delivery in freely moving animals.* J Neurosci, 2004. **24**(7): p. 1754-9.
3. Geerts, H., *alpha7 Nicotinic receptor modulators for cognitive deficits in schizophrenia and Alzheimer's disease.* Expert Opin Investig Drugs, 2012. **21**(1): p. 59-65.
4. Roberts, P.D., A. Spiros, and H. Geerts, *Simulations of symptomatic treatments for Alzheimer's disease: computational analysis of pathology and mechanisms of drug action.* Alzheimers Res Ther, 2012. **4**(6): p. 50.
5. Spiros, A. and L. Edelstein-Keshet, *Testing a model for the dynamics of actin structures with biological parameter values.* Bull Math Biol, 1998. **60**(2): p. 275-305.
6. Xiberas, X., et al., *Extrastriatal and striatal D(2) dopamine receptor blockade with haloperidol or new antipsychotic drugs in patients with schizophrenia.* Br J Psychiatry, 2001. **179**: p. 503-8.
7. Ogren, S.O., et al., *The role of 5-HT(1A) receptors in learning and memory.* Behav Brain Res, 2008. **195**(1): p. 54-77.
8. John, C.E. and S.R. Jones, *Fast Scan Cyclic Voltammetry of Dopamine and Serotonin in Mouse Brain Slices.* 2007.
9. John, C.E., et al., *Neurochemical characterization of the release and uptake of dopamine in ventral tegmental area and serotonin in substantia nigra of the mouse.* J Neurochem, 2006. **96**(1): p. 267-82.
10. Pendyam, S., et al., *Computational model of extracellular glutamate in the nucleus accumbens incorporates neuroadaptations by chronic cocaine.* Neuroscience, 2009. **158**(4): p. 1266-76.
11. Mamo, D., et al., *Differential effects of aripiprazole on D(2), 5-HT(2), and 5-HT(1A) receptor occupancy in patients with schizophrenia: a triple tracer PET study.* Am J Psychiatry, 2007. **164**(9): p. 1411-7.
12. Rasmussen, H., et al., *Serotonin2A receptor blockade and clinical effect in first-episode schizophrenia patients treated with quetiapine.* Psychopharmacology (Berl), 2011. **213**(2-3): p. 583-92.
13. Trichard, C., et al., *Binding of antipsychotic drugs to cortical 5-HT2A receptors: a PET study of chlorpromazine, clozapine, and amisulpride in schizophrenic patients.* Am J Psychiatry, 1998. **155**(4): p. 505-8.
14. Kapur, S., et al., *Reliability of a simple non-invasive method for the evaluation of 5-HT2 receptors using [18F]-setoperone PET imaging.* Nucl Med Commun, 1997. **18**(5): p. 395-9.

15. Kapur, S., et al., *Is amoxapine an atypical antipsychotic? Positron-emission tomography investigation of its dopamine2 and serotonin2 occupancy.* Biol Psychiatry, 1999. **45**(9): p. 1217-20.
16. Stark, A.D., et al., *Interaction of the novel antipsychotic aripiprazole with 5-HT1A and 5-HT 2A receptors: functional receptor-binding and in vivo electrophysiological studies.* Psychopharmacology (Berl), 2007. **190**(3): p. 373-82.
17. Sepulveda, M.I., S.C. Lummis, and I.L. Martin, *The agonist properties of m-chlorophenylbiguanide and 2-methyl-5-hydroxytryptamine on 5-HT3 receptors in N1E-115 neuroblastoma cells.* Br J Pharmacol, 1991. **104**(2): p. 536-40.
18. Leff, P., *The two-state model of receptor activation.* Trends Pharmacol Sci, 1995. **16**(3): p. 89-97.
19. Odagaki, Y. and R. Toyoshima, *5-HT1A receptor agonist properties of antipsychotics determined by [35S]GTPgammaS binding in rat hippocampal membranes.* Clin Exp Pharmacol Physiol, 2007. **34**(5-6): p. 462-6.
20. Audinot, V., et al., *Inverse agonist properties of antipsychotic agents at cloned, human (h) serotonin (5-HT)(1B) and h5-HT(1D) receptors.* Neuropsychopharmacology, 2001. **25**(3): p. 410-22.
21. Audinot, V., A. Newman-Tancredi, and M.J. Millan, *Constitutive activity at serotonin 5-HT(1D) receptors: detection by homologous GTPgammaS versus [(35)S]-GTPgammaS binding isotherms.* Neuropharmacology, 2001. **40**(1): p. 57-64.
22. Newman-Tancredi, A., et al., *Differential actions of antiparkinson agents at multiple classes of monoaminergic receptor. III. Agonist and antagonist properties at serotonin, 5-HT(1) and 5-HT(2), receptor subtypes.* J Pharmacol Exp Ther, 2002. **303**(2): p. 815-22.
23. Mikami, T., et al., *In vitro and in vivo pharmacological characterization of PF-01354082, a novel partial agonist selective for the 5-HT(4) receptor.* Eur J Pharmacol, 2009. **609**(1-3): p. 5-12.
24. Howes, O.D. and S. Kapur, *The dopamine hypothesis of schizophrenia: version III--the final common pathway.* Schizophr Bull, 2009. **35**(3): p. 549-62.
25. Corradetti, R., et al., *Differential effects of the 5-hydroxytryptamine (5-HT)1A receptor inverse agonists Rec 27/0224 and Rec 27/0074 on electrophysiological responses to 5-HT1A receptor activation in rat dorsal raphe nucleus and hippocampus in vitro.* J Pharmacol Exp Ther, 2005. **315**(1): p. 109-17.
26. Zhuang, Z.P., et al., *Derivatives of 4-(2'-methoxyphenyl)-1-[2'-(N-2"-pyridinyl-p-iodobenzamido)ethyl]pipera zine (p-MPPI) as 5-HT1A ligands.* J Med Chem, 1994. **37**(26): p. 4572-5.
27. Tan, P.Z., et al., *Characterization of radioactive metabolites of 5-HT2A receptor PET ligand [18F]altanserin in human and rodent.* Nucl Med Biol, 1999. **26**(6): p. 601-8.
28. Leysen, J.E., et al., *Receptor interactions of dopamine and serotonin antagonists: binding in vitro and in vivo and receptor regulation.* Psychopharmacol Ser, 1988. **5**: p. 12-26.
29. Marner, L., et al., *Kinetic modeling of 11C-SB207145 binding to 5-HT4 receptors in the human brain in vivo.* J Nucl Med, 2009. **50**(6): p. 900-8.
30. Burstein, E.S., et al., *Intrinsic efficacy of antipsychotics at human D2, D3, and D4 dopamine receptors: identification of the clozapine metabolite N-desmethylclozapine as a D2/D3 partial agonist.* J Pharmacol Exp Ther, 2005. **315**(3): p. 1278-87.
31. Seeman, P. and T. Tallerico, *Antipsychotic drugs which elicit little or no parkinsonism bind more loosely than dopamine to brain D2 receptors, yet occupy high levels of these receptors.* Mol Psychiatry, 1998. **3**(2): p. 123-34.
32. Durstewitz, D., J.K. Seamans, and T.J. Sejnowski, *Dopamine-mediated stabilization of delay-period activity in a network model of prefrontal cortex.* J Neurophysiol, 2000. **83**(3): p. 1733-50.
33. DeFelipe, J., *Cortical interneurons: from Cajal to 2001.* Prog Brain Res, 2002. **136**: p. 215-38.

34. Sidiropoulou, K., et al., *Dopamine modulates an mGluR5-mediated depolarization underlying prefrontal persistent activity.* Nat Neurosci, 2009. **12**(2): p. 190-9.
35. Isaacson, J.S. and M. Scanziani, *How inhibition shapes cortical activity.* Neuron, 2011. **72**(2): p. 231-43.
36. Levy, R. and P.S. Goldman-Rakic, *Segregation of working memory functions within the dorsolateral prefrontal cortex.* Exp Brain Res, 2000. **133**(1): p. 23-32.
37. Law-Tho, D., J.C. Hirsch, and F. Crepel, *Dopamine modulation of synaptic transmission in rat prefrontal cortex: an in vitro electrophysiological study.* Neurosci Res, 1994. **21**(2): p. 151-60.
38. Tseng, K.Y. and P. O'Donnell, *D2 dopamine receptors recruit a GABA component for their attenuation of excitatory synaptic transmission in the adult rat prefrontal cortex.* Synapse, 2007. **61**(10): p. 843-50.
39. Yuen, E.Y. and Z. Yan, *Dopamine D4 receptors regulate AMPA receptor trafficking and glutamatergic transmission in GABAergic interneurons of prefrontal cortex.* J Neurosci, 2009. **29**(2): p. 550-62.
40. Foehring, R.C., *Serotonin modulates N- and P-type calcium currents in neocortical pyramidal neurons via a membrane-delimited pathway.* J Neurophysiol, 1996. **75**(2): p. 648-59.
41. Cardenas, C.G., L.P. Del Mar, and R.S. Scroggs, *Two parallel signaling pathways couple 5HT1A receptors to N- and L-type calcium channels in C-like rat dorsal root ganglion cells.* J Neurophysiol, 1997. **77**(6): p. 3284-96.
42. Gerhardt, C.C. and H. van Heerikhuizen, *Functional characteristics of heterologously expressed 5-HT receptors.* Eur J Pharmacol, 1997. **334**(1): p. 1-23.
43. Carr, D.B., et al., *Serotonin receptor activation inhibits sodium current and dendritic excitability in prefrontal cortex via a protein kinase C-dependent mechanism.* J Neurosci, 2002. **22**(16): p. 6846-55.
44. Puig, M.V., et al., *In vivo excitation of GABA interneurons in the medial prefrontal cortex through 5-HT3 receptors.* Cereb Cortex, 2004. **14**(12): p. 1365-75.
45. Ansanay, H., et al., *cAMP-dependent, long-lasting inhibition of a K+ current in mammalian neurons.* Proc Natl Acad Sci U S A, 1995. **92**(14): p. 6635-9.
46. Cai, X., et al., *Activity-dependent bidirectional regulation of GABA(A) receptor channels by the 5-HT(4) receptor-mediated signalling in rat prefrontal cortical pyramidal neurons.* J Physiol, 2002. **540**(Pt 3): p. 743-59.
47. Riemer, C., et al., *Influence of the 5-HT6 receptor on acetylcholine release in the cortex: pharmacological characterization of 4-(2-bromo-6-pyrrolidin-1-ylpyridine-4-sulfonyl)phenylamine, a potent and selective 5-HT6 receptor antagonist.* J Med Chem, 2003. **46**(7): p. 1273-6.
48. Boehm, S., *Presynaptic alpha2-adrenoceptors control excitatory, but not inhibitory, transmission at rat hippocampal synapses.* J Physiol, 1999. **519 Pt 2**: p. 439-49.
49. Perez-Rosello, T., et al., *Cholinergic control of firing pattern and neurotransmission in rat neostriatal projection neurons: role of CaV2.1 and CaV2.2 Ca2+ channels.* J Neurophysiol, 2005. **93**(5): p. 2507-19.
50. Shen, W., et al., *Cholinergic suppression of KCNQ channel currents enhances excitability of striatal medium spiny neurons.* J Neurosci, 2005. **25**(32): p. 7449-58.
51. Parnas, H., et al., *Depolarization initiates phasic acetylcholine release by relief of a tonic block imposed by presynaptic M2 muscarinic receptors.* J Neurophysiol, 2005. **93**(6): p. 3257-69.
52. Zhang, W., et al., *Multiple muscarinic acetylcholine receptor subtypes modulate striatal dopamine release, as studied with M1-M5 muscarinic receptor knock-out mice.* J Neurosci, 2002. **22**(15): p. 6347-52.

53. Parikh, V., et al., *Prefrontal beta2 subunit-containing and alpha7 nicotinic acetylcholine receptors differentially control glutamatergic and cholinergic signaling.* J Neurosci, 2010. **30**(9): p. 3518-30.
54. Alkondon, M. and E.X. Albuquerque, *Nicotinic acetylcholine receptor alpha7 and alpha4beta2 subtypes differentially control GABAergic input to CA1 neurons in rat hippocampus.* J Neurophysiol, 2001. **86**(6): p. 3043-55.
55. Aracri, P., et al., *Tonic modulation of GABA release by nicotinic acetylcholine receptors in layer V of the murine prefrontal cortex.* Cereb Cortex, 2010. **20**(7): p. 1539-55.
56. Tamminga, C.A. and A. Carlsson, *Partial dopamine agonists and dopaminergic stabilizers, in the treatment of psychosis.* Curr Drug Targets CNS Neurol Disord, 2002. **1**(2): p. 141-7.
57. Sun, X., Y. Zhao, and M.E. Wolf, *Dopamine receptor stimulation modulates AMPA receptor synaptic insertion in prefrontal cortex neurons.* J Neurosci, 2005. **25**(32): p. 7342-51.
58. Moghaddam, B., *Recent basic findings in support of excitatory amino acid hypotheses of schizophrenia.* Prog Neuropsychopharmacol Biol Psychiatry, 1994. **18**(5): p. 859-70.
59. Coyle, J. and G. Tsai, *The NMDA receptor glycine modulatory site: a therapeutic target for improving cognition and reducing negative symptoms in schizophrenia.* Psychopharmacology, 2003. **174**(1).
60. Meyer-Lindenberg, A., et al., *Reduced prefrontal activity predicts exaggerated striatal dopaminergic function in schizophrenia.* Nat Neurosci, 2002. **5**(3): p. 267-71.
61. Volk, D.W. and D.A. Lewis, *Impaired prefrontal inhibition in schizophrenia: relevance for cognitive dysfunction.* Physiol Behav, 2002. **77**(4-5): p. 501-5.
62. Winterer, G., et al., *Schizophrenia: reduced signal-to-noise ratio and impaired phase-locking during information processing.* Clin Neurophysiol, 2000. **111**(5): p. 837-49.
63. Saykin, A.J., et al., *Neuropsychological deficits in neuroleptic naive patients with first-episode schizophrenia.* Arch Gen Psychiatry, 1994. **51**(2): p. 124-31.
64. Kurtz, M.M., et al., *Approaches to cognitive remediation of neuropsychological deficits in schizophrenia: a review and meta-analysis.* Neuropsychol Rev, 2001. **11**(4): p. 197-210.
65. Elvevag, B. and T.E. Goldberg, *Cognitive impairment in schizophrenia is the core of the disorder.* Crit Rev Neurobiol, 2000. **14**(1): p. 1-21.
66. Bertolino, A., et al., *Interaction of COMT (Val(108/158)Met) genotype and olanzapine treatment on prefrontal cortical function in patients with schizophrenia.* Am J Psychiatry, 2004. **161**(10): p. 1798-805.
67. Weickert, T.W., et al., *Catechol-O-methyltransferase val108/158met genotype predicts working memory response to antipsychotic medications.* Biol Psychiatry, 2004. **56**(9): p. 677-82.
68. Green, A., et al., *Muscarinic and nicotinic receptor modulation of object and spatial n-back working memory in humans.* Pharmacol Biochem Behav, 2005. **81**(3): p. 575-84.
69. Roussos, P., S.G. Giakoumaki, and P. Bitsios, *Tolcapone effects on gating, working memory, and mood interact with the synonymous catechol-O-methyltransferase rs4818c/g polymorphism.* Biol Psychiatry, 2009. **66**(11): p. 997-1004.
70. Box, H.C., E.E. Budzinski, and H.G. Freund, *Studies of electrons trapped in X-irradiated rhamnose crystals.* Radiat Res, 1990. **121**(3): p. 262-6.
71. Watts, A., M. Watts, and J. Snelling, *Seeds of genius : the early writings of Alan Watts*. 1997, Shaftesbury, Dorset ; Rockport, Mass: Element Books. viii, 312 p.